horticulturae

MDPI

Article

Molecular Characterization of Terpenoid Biosynthetic Genes and Terpenoid Accumulation in *Phlomis umbrosa* Turczaninow

Si-Yoon Hwang [1,†], Sang-Hoon Lee [1,†], Young-Seob Lee [1], Sin-Hee Han [1], Beom-Heon Song [2], Chinreddy Subramanyam Reddy [1], Yeon Bok Kim [1,3,*] and Sang Un Park [4,5,*]

1 Department of Herbal Crop Resources, National Institute of Horticultural & Herbal Science, RDA, Eumseong-gun, Chungcheongbuk-do 369-873, Korea; chocobosea12@gmail.com (S.-Y.H.); omega119@korea.kr (S.-H.L.); youngseoblee@korea.kr (Y.-S.L.); herbman@korea.kr (S.-H.H.); suumani@gmail.com (C.S.R.)

2 Department of Agronomy Graduate School, Chungbuk National University Cheongju, Heungdeok 28644, Korea; bhsong@chungbuk.ac.kr

3 Department of Medicinal and Industrial Crops, Korean National College of Agriculture and Fisheries, Jeonju 54874, Korea

4 Department of Crop Science, Chungnam National University, 99 Daehak-ro, Yuseong-gu, Daejeon 34134, Korea

5 Department of Smart Agriculture Systems, Chungnam National University, 99 Daehak-Ro, Yuseong-gu, Daejeon 34134, Korea

* Correspondence: yeondarabok@korea.kr (Y.B.K.); supark@cnu.ac.kr (S.U.P.); Tel.: +82-63-238-9092 (Y.B.K.); +82-42-821-5730 (S.U.P.); Fax: +82-63-238-9099 (Y.B.K.); +82-42-822-2631 (S.U.P.)

† Si-Yoon Hwang and Sang-Hoon Lee contributed equally to this work.

Received: 3 September 2020; Accepted: 2 November 2020; Published: 5 November 2020

Abstract: The root of *Phlomis umbrosa* has traditionally been used as a medicine in South Asian nations to treat colds and bone fractures, to staunch bleeding, and as an anti-inflammatory, and such use continues today. We identified 10 genes that are involved in terpenoid biosynthesis, while using the Illumina/Solexa HiSeq2000 platform. We investigated the transcript levels of the 10 genes using quantitative real-time PCR and quantified the level of terpenoid accumulation in different organs of *P. umbrosa* while using high-performance liquid chromatography. The transcript levels of *PuHDR* and *PuHMGR1* were the highest among the studied genes. Sesamoside, an iridoid glycoside, appeared in higher quantity than shanzhiside methylester, umbroside (8-O-acetyl shanzhiside methyl ester), and acteoside. We speculate that *PuHDR* and *PuHMGR1* may contribute to terpenoid biosynthesis in *P. umbrosa*. This study highlights the molecular mechanisms that underlie iridoid glycoside biosynthesis in *P. umbrosa*.

Keywords: *Phlomis umbrosa*; terpenoid; transcript level

1. Introduction

Phlomis umbrosa Turczaninow is a perennial herbaceous plant species in the Lamiaceae family; the genus *Phlomis* contains hundreds of species across Africa, Europe, and Asia [1]. The aerial parts of some species have been used in herbal teas, and the roots of *P. umbrosa* have been used as a traditional medicine for a long time. Preparations of *P. umbrosa* are considered as potential therapeutic drugs to treat bone fractures, rheumatic diseases, and cold; to reduce swelling; and, to staunch bleeding in South Asian countries, particularly in Korea, China, and Japan [2,3]. The plant contains triterpenoids, iridoid glycosides, and phenylethanoid glycosides [4], and it has been used in anti-allergic,

anti-inflammatory, and anti-nociceptive treatment [5,6]. *P. umbrosa* has two types of flowers: they appear in different plants (photo in Figure 1).

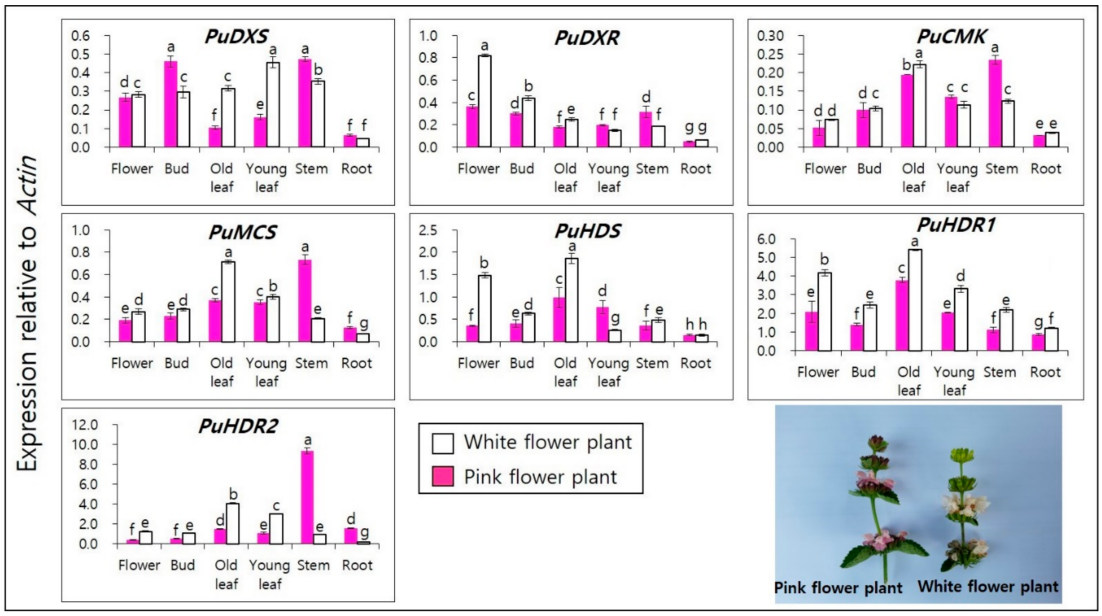

Figure 1. Expression levels of *PuDXS*, *PuDXR*, *PuCMK*, *PuMCS*, *PuHDS*, and *PuHDRs* in the flowers, buds, leaves (old and young), stem, and root of *P. umbrosa*. The height of each bar and the error bars show the mean and standard error, respectively, from three independent measurements. The values indicate means ± SD. Means with different letters are significant at $p < 0.05$ by Duncan's Multiple Range Test (DMRT).

Terpenoids belong to a large cluster of terpene-derived secondary metabolites that are formed through two metabolic pathways in plants. The mevalonic acid (MVA) pathway is the first to be formed, later becoming the 2-C-methyl-D-erythritol 4-phosphate (MEP) pathway. Terpenoids are primarily categorized by their number of isoprene units, and then categorized into hemiterpenoids (one isoprene unit with five carbons), monoterpenoids (two isoprene units with 10 carbons), sesquiterpenoids (three isoprene units with 15 carbons), diterpenoids (four isoprene units with 20 carbons), triterpenoids (six isoprene units with 30 carbons), tetraterpenoids (eight isoprene units with 40 carbons), and polyterpenoids ((C_5)n with n > 8) [7]. Iridoids are derived from monoterpenes, which are typically found in plants as glycosides. Many iridoid glycosides have been isolated in *P. umbrosa*, including asacteoside, asperuloside, aucubin, feretoside, geniposide, sesamoside, shanzhiside methylester, ixoroside, and ixoside and others [8–10]. To date, iridoid glycosides have been shown to have anti-inflammatory, anti-fibrinolytic, and neuroprotective effects [11–13].

For differential gene expression analysis of pink and white flowers of *P. umbrosa*, we used the RNA-Seq method to produce a large number of transcriptome sequences with an Illumina Hi-Seq 2000 platform. We isolated ten genes that were involved in the terpenoid biosynthesis pathway, six of which DXS (1-Deoxy-D-xylulose 5-phosphate synthase), DXR (1-Deoxy-D-xylulose 5-phosphate reductoisomerase), CMK (4-diphosphocytidyl-2-C-methyl-D-erythritol kinase), HDS ((E)-4-Hydroxy -3-methyl-but-2-enyl pyrophosphate synthase), HDR ((E)-4-Hydroxy-3-methyl-but-2-enyl pyrophosphate synthase reductase)), and MCS (2-C-methyl-d-erythritol 2,4 cyclodiphosphate synthase) belong to the non-mevalonate (MEP) pathway. HMGR (3-hydroxy-3-methylglutaryl-coenzyme A reductase), MK (mevalonate kinase), PMK (5-phosphomevalonate kinase), and MVD (mevalonate diphosphate decarboxylase)) belong to the mevalonate (MVA) pathway. Terpenoid biosynthesis usually occurs in the MVA and MEP pathways, which generate the same products, but at different locations, i.e., isopentenyl diphosphate (IPP) through MVA in the cytosol and dimethylallyl diphosphate (DMAPP)

through MEP in the plastid [14]. Pyruvate and glyceraldehyde 3-phosphate (G3P) are precursors of MEP. DXS is the initial enzyme that enables the creation of DXP (1-Deoxy-D-xylulose 5-phosphate) from pyruvate and G3P condensation. DXR is the enzyme that converts DXP into MEP. CMS (2-C-methyl-D-erythritol 4-phosphate cytidylyl transferase) and CMK assist in the conversion of MEP to CDP-MEP (4-diphosphocytidyl-2-C-methyl-D-erythritol 2-phosphate). MCS facilitates the generation of MEcPP (2-C-methyl-D-erythritol 2,4-cyclodiphosphate) and, thereafter, HDS adapts the MEcPP to HMBPP ((E)-4-Hydroxy-3-methyl-but-2-enyl pyrophosphate). Ultimately, HDR aids in generating IPP and DMAPP. Another pathway, MVA, starts with acetyl-CoA. AACT (Acetoacetyl-CoA thiolase) is the first enzyme that helps generate acetoacetyl-CoA from molecular condensation of 2 acetyl-CoA. HMG-CoA synthase helps to produce HMG-CoA from acetoacetyl-CoA and acetyl-CoA condensation. HMGR converts HMG-CoA into MVA. MK and PMK help convert MVA into MVAPP through the phosphorylation process. Finally, MVD helps to generate IPP from the decarboxylation of MVAPP (Scheme 1).

Several studies have investigated the accumulation of terpenoids and the transcription regulation of their related genes in plants [15–18]. However, the gene expression and characterization of terpenoid compounds in different tissues of *P. umbrosa* have not yet been published. Thus, we studied the accumulation of terpenoids and their related genes in the transcriptional regulation of different organs of *P. umbrosa*.

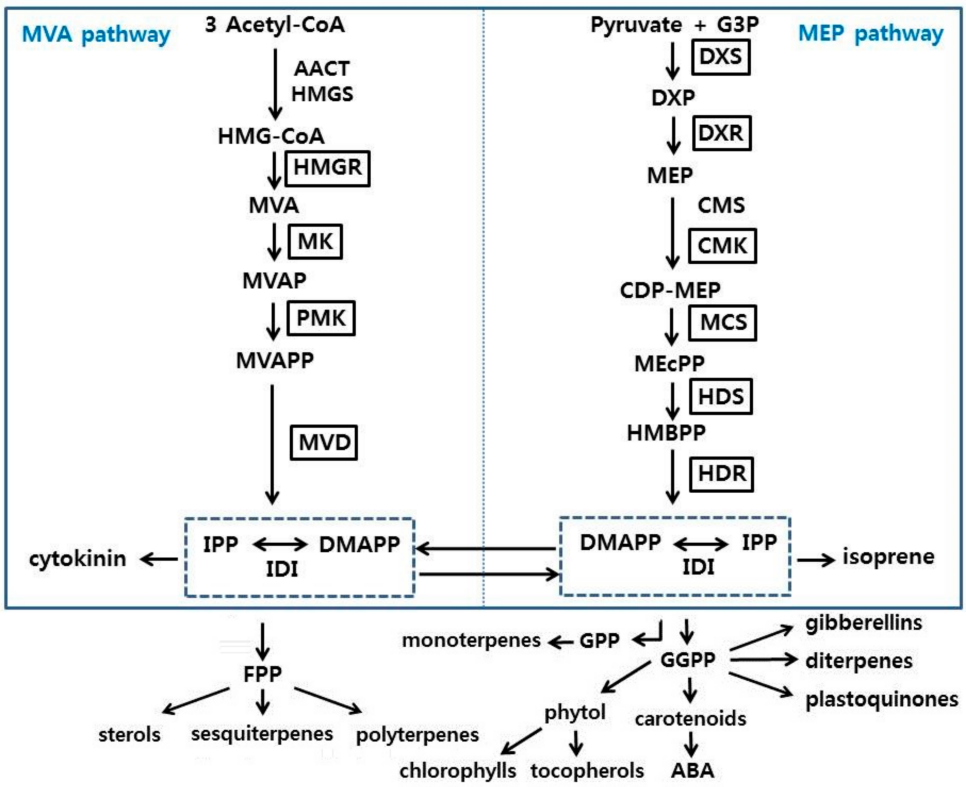

Scheme 1. Schematic representation of terpenoid biosynthesis in plants [19]. Terpenoids and their biosynthetic enzymes were analyzed in this study, and the analyzed enzyme is indicated with black boxes.

2. Materials and Methods

2.1. Plant Materials

P. umbrosa specimen plants were established in the experimental field of the National Institute of Horticultural and Herbal Science, Rural Development Administration (Eumseong, Korea). Samples of flowers, stems, leaves, and roots were collected from 15 healthy plants, white and pink type plants,

respectively, and immediately freeze-dried with liquid nitrogen, then stored at −80 °C until use. The samples were used for RNA extraction and HPLC ultraviolet analysis. All of the experiments were performed with at least three biological replicates.

2.2. Total RNA Isolation and Quantitative Real-Time PCR (qRT-PCR)

The total RNA from each individual sample was extracted using an RNeasy total RNA kit (Qiagen, Hilden, Germany), following the manufacturer's protocol. RNAse-Free DNase Set (cat. no. 79254) was used to digest contaminating DNA in RNA solutions prior to RNA cleanup. The quantity of RNA was computed on a NanoVuePlus spectrophotometer (GE Healthcare Life Sciences, Logan, UT, USA), and the quality was verified by adding 1 µg of the RNA to a 1.2% formaldehyde RNA agarose gel. Subsequently, 1 µg of total RNA was reverse-transcribed while using the SuperScript™ double-stranded synthesis kit (Invitrogen, Carlsbad, CA, USA) following the manufacturer's protocol. For qRT-PCR, the cDNA was diluted 20-fold. The reaction volume was 20 µL comprising 0.5 µM primers and 2× real-time PCR Smart mix (SolGent, Daejeon, Korea). qRT-PCR was performed while using three independent biological replicates with a BIO-RAD CFX96 real-time PCR system (Bio-Rad Laboratories, Hercules, CA, USA) under the following conditions: initial denaturation at 95 °C for 15 min. followed by 40 cycles of denaturation at 95 °C for 20 s, annealing at 55 °C for 40 s, and extension at 72 °C for 20 s. Actin gene (GenBank accession no. KU317507) was used as the reference gene.

2.3. Next Generation Sequencing of Transcriptome

We implemented Illumina-based NGS sequencing in order to obtain high-throughput transcriptome data of *P. umbrosa*. The total RNAs were quantified using Nanodrop spectrophotometer (Thermo Scientific, Waltham, MA, USA) and quality-assessed by RNA 6000 Nano assay kit (Agilent, Santa Clara, CA, USA) and Bioanalyser 2100 (Agilent). NGS sequencing libraries were generated from one microgram of total RNA using Truseq RNA Sample Prep Kit (Illumina, San Diego, CA, USA) according to the manufacturer's protocol. In brief, the poly-A containing RNA molecules were purified while using poly-T oligo attached magnetic beads. After purification, the total poly A+ RNA was fragmented into small pieces using divalent cations under elevated temperature. The cleaved mRNA fragments were reverse transcribed into first strand cDNA using random primers. QiaQuick PCR extraction kit was used for the purification of the shorts fragments and further resolved with EB buffer for end reparation and addition of poly (A). After that, the short fragments with poly (A) tail were interlinked with sequencing adapters. Each library was separated by adjoining distinct MID tag. The resulting cDNA libraries were then paired-end sequenced (2 × 101 bp) with the Illumina HiSeq™ 2000 system.

2.4. Sequence Analysis

P. umbrosa terpenoid biosynthetic pathway genes and the deduced amino acid sequences were aligned while using the Biological Sequence Alignment Editor (BioEdit). Protein molecular weight and isoelectric point values were measured using the Compute pI/Mw tool (ExPASy, http://ca.expasy.org/tools/pi_tool.html). Terpenoid biosynthesis pathway gene-specific primers were created using an online program (https://www.genscript.com/ssl-bin/app/primer) (Table 1).

Table 1. Primers that were used in this study.

Primer Name	Sequence (5′ → 3′)	Size (bp)	GenBank Access. No.
PuDXS (F) *PuDXS (R)*	ACGGGCATGAACCTCTTCCA GATGCCTTCACAGGCCAACC	108	KU317508
PuDXR (F) *PuDXR (R)*	TCCAAGGTGGATTGCCTTTGAA GTTTCGGGCCATCCCAAGTT	147	KU317509
PuCMK (F) *PuCMK (R)*	CTGCTACGCTCCCAACAACG AGCGGTGGCTTTGATCGAATA	148	MK482372
PuMCS (F) *PuMCS (R)*	GCTGCTGCCTCAAGCACTGT GAGCCGGTGAAGGTCGAATC	105	MK482371
PuHDS (F) *PuHDS (R)*	GGTCTCAAAACCAGGGATCA TAGCAATGGGCTTCCTTCAG	180	MK482373
PuHDR1 (F) *PuHDR1 (R)*	GGCCATCTCTCTGCAATTCT TTGCTCCTCGTCAAGTTGTG	180	MK482374
PuHDR2 (F) *PuHDR2 (R)*	ATGGCGATTTCTCTGCAGTT CCCCTTGCGATTGTAGTTGT	207	MK482375
PuHMGR1 (F) *PuHMGR1 (R)*	CGCCTACTTTCTGCTTCACC ATGTTCCGATCTTCGTGGAG	216	KU317502
PuHMGR2 (F) *PuHMGR2 (R)*	CACCCCTCTCCACATCCTTA GCGTGTATCTTCGTTCAGCA	190	KU317501
PuMK (F) *PuMK (R)*	CCTACTCCCGAGGAAAATGAT TGGCCTCGAATGAACATGATA	151	KU317505
PuPMK (F) *PuPMK (R)*	CCAAATGCCGGGATTGTACTG TGGCCATCTGAGGAGAAGTGAG	129	KU317506
PuMVD (F) *PuMVD (R)*	GCGATAGCATTGCTGTTCAA ATCGCGCTTTTGTATTGCTT	209	KU317504
PuActin (F) *PuActin (R)*	TCCAGCCTTCATTGATCGGAA GGTCAGCGATACCAGGGAACA	150	KU317507

2.5. Isolation and HPLC Analysis of P. umbrosa Terpenoids

Terpenoids were analyzed with HPLC following a previously published protocol, with minor amendments [20]. The samples were freeze-dried and ground into a fine powder. Each sample (100 mg dry weight (DW)) was extracted while using 10 mL of 100% methanol (MeOH). This step was performed under vortexing for 5 min. at room temperature, and then, the sample was extracted for 1 h at 37 °C, with 1 min. of vortexing every 20 min. After centrifugation at 1000× *g* for 5 min, the supernatant was filtered and used for analysis. External standards were procured from Chemfaces (Wuhan, HB, China). MeOH, acetonitrile, and phosphoric acid were purchased from Wako Pure Chemical Industries (Osaka, Japan) and Junsei Chemical Co., Ltd. (Kyoto, Japan), respectively. The extract was filtered through a 0.45-µm poly-filter and then diluted two-fold with MeOH prior to HPLC analysis. Terpenoids were detected in a C18 column (250 × 4.6 mm, 5 µm; Shisido Company, Tokyo, Japan) by Agilent 1100 HPLC (Santa Clara, CA, USA), provided with a photodiode array (PDA) detector. The detection range for terpenoids was 235 nm in the chromatograms. Solvent A (100% acetonitrile) and solvent B (water/phosphoric acid at 99.5:0.5 *v*/*v*) were used as the mobile phase. The injection volume was 20 µL and the column was maintained at 30 °C. Gradient elution analysis (1 mL/min.) was accomplished by maintaining the following conditions: A 5%, B 95%, 0 min; A 17%, B 83%, 20 min; A 22%, B 78%, 30 min; A 30%, B 70%, 40 min; A 5%, B 95%, 41 min; and, A 5%, B 95%, 45 min.

2.6. Statistical Analysis

Statistical analyses were performed while using SAS Enterprise Guide 4.2 (Statistical analysis system, Cray, NC, USA, 2009) software. The data provided in this study are the mean and standard deviation of multiple replicates, with a minimum of three samples. Duncan's Multiple Range Test (DMRT) at $p < 0.05$ determined variations between the means.

3. Results

3.1. Sequencing and Transcriptome Assembly

cDNAs prepared from root of *P. umbrosa* were sequenced using Illumina Hiseq platform. As a result of sequencing, 21,281,712 of total raw reads were obtained from sample. In order to facilitate sequence assembly, these reads were assembled using Velvet and Oases assembly program, resulting in 149,488 contigs with an average contig length of 1231 nt and an N50 of 1935 nt, ranging from 500 nt to >4000 nt. Furthermore, Velvet and Oases were used for assembling 75,392 unigenes with a mean size of 849 nt and an N50 of 1422 nt (Table 2).

Table 2. Summary of the transcriptome of *P. umbrosa.*

	Total Number	Total Nucleotides (nt)	Mean Length (nt)	N50
Total raw reads	21,281,712	-	-	-
Total Contigs	149,488	184,148,836	1231	1935
Total unigenes	75,392	64,062,377	849	1422

3.2. Isolation and Sequence Analysis of Terpenoid Biosynthetic Genes from P. umbrosa

Twelve genes (*PuDXS, PuDXR, PuCMK, PuMCS, PuHDS, PuHDR1*, and *PuHDR2* in the MEP pathway and *PuHMGR1, PuHMGR2, PuMK, PuPMK*, and *PuMVD* in the MVA pathway) associated with terpenoid biosynthesis in *P. umbrosa* were identified while using NGS, Illumina/Solexa HiSeq2000 platform. The open reading frame (ORF) of *PuDXS* was 2148 base pairs (bp) and encoded a protein with 715 amino acids (aa), a theoretical molecular weight (MW) of 76.82 kDa, and an assumed isoelectric point value (pI) of 6.59. *PuDXS* showed high homology (85–90%) with DXS genes from other plants based on NCBI BLAST analysis of the deduced amino acid sequences; it showed a preserved motif (HPFSKNYEARKGSTGICASLSERGE) that lies between amino acid positions 37 to 61, which were common to other plants (Supplementary Figure S1). In addition, the thiamin diphosphate binding domain (GDGAMTAGQAYEAMNNAGYLDSDMIVILNDN) was also found in *PuDXS* [21]. The partial *PuDXR* had 1406 bps and 468 aa. The predicted MW was 50.98 kDa and the estimated pI value was 6.09. It showed high homology (85–90%) with DXR genes from other plants (Supplementary Figure S2). The preserved motif (CSA; PPAWPGRAV) and NADPH binding domain (GSTGSIG) were also observed in *PuDXR* [22]. The fractional *PuCMK* had 1055 bp and 351 aa, with a predicted MW of 38.02 kDa and a deduced pI of 9.14. It included an ATP binding domain (DKKVPTGAGLGGGSSNAATAL) (Supplementary Figure S3) [23]. Furthermore, fractional *PuMCS* had 711 bp and 236 aa, with a predicted MW of 25.05 kDa and deduced pI of 8.33. It also expressed a magnesium/manganese ion binding site (Supplementary Figure S4) [24]. The partial *PuHDS* had 2229 bp and 742 aa, with a predicted MW of 82.58 kDa and a deduced pI of 6.19. It produced high similarity (87–92%) with HDS genes from other plants (Supplementary Figure S5). The preserved motif (GCXVNXXGE; x being designated for any amino acid) was also observed in *PuDXR* [25]. The ORFs of *PuHDS1* and partial *PuHDS2* were 1443 and 1380 bp long, respectively, and encoded 480 and 459 aa, respectively. The predicted MWs of *PuHDS1* and *PuHDS2* were 54.89 and 51.85 kDa, respectively, and the deduced pI values were 6.23 and 5.62, respectively. These illustrated an N-terminal conserved domain and exhibited 78–82% homology with the HDS genes of other plants (Supplementary Figure S6) [26].

The ORFs of PuHMGR1 and partial PuHMGR2 were 1698 and 1438 bp and encoded 565 and 479 amino acids; the predicted MWs were 60.78 and 51.66 kDa, respectively. The predicted pI values were 7.50 and 5.04, respectively. These included preserved motifs (EMPVGF; IVSAVFIATGQ) and NAD(P) H-binding domains (TGDAMGMNMVS; VGTVGG) (Supplementary Figure S7) [27]. The PuMK had 1164 bp and 387 aa, with a predicted MW of 41.17 kDa and predicted pI of 5.45. It demonstrated high similarity (81–87%) with the MK genes of other plants. The protein sequence confirmed three conserved motifs (PGKIILAGEH, PLGSGLGSSAA, and KLTGAGGGGC) (Supplementary Figure S8) [28]. The PuPMK was 1515 bp long and it restrained 504 aa. The estimated MW and predicted pI value were 54.42 kDa and 5.25, respectively. It also contained three conserved motifs (GKVLMTGGY, GLGSSAA, and LLGEPGAGGS) (Supplementary Figure S9) [29]. The terminal gene (PuMVD) in the MVA pathway comprised 1269 bp and 422 aa, with a predicted MW of 46.78 kDa and predicted pI value of 6.33. It showed high homology (82–92%) with MVD genes of other plants. The preserved motifs (DRMWLNGK, RFQNCLRELR, NNFPTAAGL, and ASSAAGLAC) and an ATP binding domain (NNFPTAAGLASSAAGLAC) were also found in PuMVD (Supplementary Figure S10) [30].

3.3. Terpenoid Biosynthetic Genes Spatial Expression Profiles in of P. umbrosa

The expression profiles of *PuDXS*, *PuDXR*, *PuCMK*, *PuMCS*, *PuHDS*, and *PuHDRs* in the flower, bud, leaf, stem, and root tissues of *P. umbrosa* were analyzed while using qRT-PCR (Figure 1). All the studied genes were expressed differently in different organs (i.e., flower, bud, leaf, and stem), and minimal expression profiles were noted in the root tissue. The initial enzyme *PuDXS* demonstrated less than 0.5-fold expression in most of the organs, but the expression level was high in the bud and stem tissues of pink flowers, as well as in the leaves of white-flowering plants. *PuDXR* showed the highest level of expression (0.8-fold) in the flower parts of white flowers, whereas it yielded less than 0.5-fold in other organs. *PuCMK* and *PuMCS* expressed a similar pattern, but the expression level was high in the old leaves of the white flowering plants and in the stems of the pink flowering plants. *PuHDS* showed the highest expression level in white flowering plants in all organs, except for young leaves. The terminal enzymes *PuHDR*1,2 showed the highest expression levels among the studied genes. The expression profile of *PuHDR1* was greater than five-old in the old leaves of white flowering plants, whereas *PuHDR2* expression was greater than nine-fold in the stem of the pink flowering plants.

Similarly, the expression patterns of *PuHMGRs*, *PuMK*, *PuPMK*, and *PuMVD* were evaluated in different parts of both color variants while using qRT-PCR (Figure 2). All five genes were highly expressed in the roots and stems. The expression levels were higher in pink flowers than in white flowers, and in the pink flowering plants, all genes except *PuMVD* showed higher gene expression profiles in the stem than the roots. *PuHMGR1* showed the highest expression levels across all tissue types.

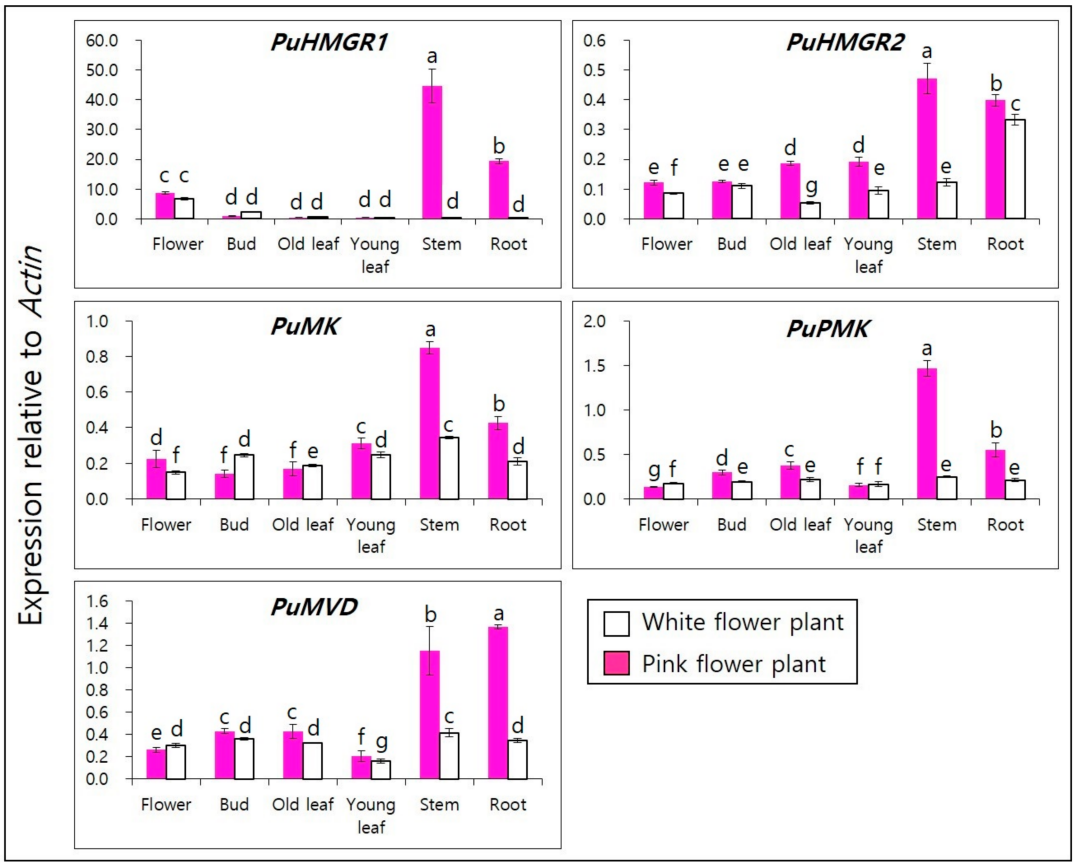

Figure 2. Expression levels of *PuHMGRs, PuMK, PuPMK*, and *PuMVD* in the flowers, buds, leaves (old and young), stem, and root of *P. umbrosa*. The height of each bar and the error bars show the mean and standard error, respectively, from three independent measurements. Values indicate means ± SD. Means with different letters are significant at $p < 0.05$ by Duncan's Multiple Range Test (DMRT).

3.4. Terpenoid (Iridoid Glycosides) Analysis in Different Organs of P. umbrosa by HPLC

The terpenoids sesamoside, shanzhiside methylester, umbroside, and acteoside were quantitatively computed and analyzed in the different organs of *P. umbrosa* while using HPLC (Table 3). Sesamoside and shanzhiside methylester levels were the highest in the roots, umbroside was highest in the leaves, and acteoside was highest in the buds. The sesamoside contents in the roots of white flowering plants (133.78 ± 1.38 μg/mg dry weight [DW]) and the roots of pink flowering plants (116.10 ± 0.48 μg/mg DW) were 2–12-fold higher than those in other organs. The shanzhiside methylester content of the white flowering plant root (16.12 ± 0.17 μg/mgDW) was five-fold higher than that of pink flowering plant roots (3.00 ± 0.01 μg/mg DW). In particular, the umbroside content of the white flowering plant roots (11.07 ± 0.13 μg/mg DW) was similar to that of the old leaves (10.79 ± 0.04 μg/mgDW) and that of young leaves (11.37 ± 0.10 μg/mgDW). However, the umbroside content of the pink flower plant roots (12.91 ± 0.04 μg/mgDW) was 0.7- and 0.5-fold lower than those of the old leaves (18.47 ± 0.25 μg/mgDW) and young leaves (25.73 ± 0.10 μg/mgDW), respectively. The acteoside content of the white flowering plant buds (62.70 ± 0.64 μg/mgDW) and pink flowering plant buds (44.14 ± 0.92 μg/mgDW) was 2.5–32 fold greater than those of other organs. When the leaves of *S. indicum* and *P. umbrosa* were compared, the content of sesamoside was higher in *P. umbrosa*, but the content of shanzhiside methylester and acteoside was higher in *S. indicum*.

Table 3. The accumulation of terpenoid (iridoid glycosides) in different organs of different flower type plant.

Type	Organ	Sesamoside	Shanzhiside Methylester	Umbroside	Acteoside
White flower plant	Flower	40.68 ± 0.10h	1.10 ± 0.01h	0.70 ± 0.00i	18.58 ± 0.04c
	Bud	49.94 ± 0.35e	1.58 ± 0.04f	1.30 ± 0.02h	62.70 ± 0.64a
	Young leaf	45.50 ± 0.01f	0.49 ± 0.01j	11.37 ± 0.10d	6.48 ± 0.83d
	Old leaf	36.75 ± 0.27i	1.72 ± 0.01e	10.79 ± 0.04f	1.62 ± 0.35ef
	Stem	11.60 ± 0.12k	0.65 ± 0.01i	0.63 ± 0.00i	0.20 ± 0.00g
	Root	133.78 ± 1.38a	16.12 ± 0.17a	11.07 ± 0.13e	0.81 ± 0.01fg
Pink flower plant	Flower	59.64 ± 0.72c	2.37 ± 0.08c	1.15 ± 0.02h	17.92 ± 0.25c
	Bud	54.58 ± 0.79d	1.43 ± 0.08g	2.00 ± 0.03g	44.14 ± 0.92b
	Young leaf	43.08 ± 0.23g	0.53 ± 0.01j	25.73 ± 0.10a	5.70 ± 0.78d
	Old leaf	36.43 ± 0.41i	1.91 ± 0.05d	18.47 ± 0.25b	2.24 ± 0.24e
	Stem	16.03 ± 0.23j	0.71 ± 0.01i	0.31 ± 0.00j	0.40 ± 0.01g
	Root	116.10 ± 0.48b	3.00 ± 0.01b	12.91 ± 0.04c	1.46 ± 0.01ef

Accumulation of terpenoid compounds in flower, bud, leaf (old and young), stem and root of *P. umbrosa*. (μg/mg DW); Each value is the mean of three replications ± standard deviation; Means with difference letters are significantly different at $p < 0.05$ by Duncan's Multiple Range Test (DMRT).

4. Discussion

Several reports have suggested that terpenoid biosynthetic genes are differentially expressed in different plant tissues. In a recent study, the genes *OfDXS1, OfDXS2,* and *OfHDR1* in *Osmanthus fragrans* were found to have higher levels of expression in the inflorescence than in other organs [31]. In a study of *Nicotiana sylvestris*, the gene *NsyCMS* was expressed in all organs, but the level of expression was the highest in the leaves of seedlings [32]. Most of the genes in the MVA pathway of *Valeriana fauriei* were expressed at the highest levels in the stem [33]. In *P. umbrosa*, the genes *PuHDR1* and *PuHMGR2* were expressed in all of the tissues, but the highest levels were observed in the leaves, stems, and roots.

Gene expression levels that are related to the biosynthetic pathways of terpenoid compounds (MVA and MEP pathways) have been reported for *V. fauriei* [33]. However, the metabolism of terpenoids has not been reported for *P. umbrosa*. This study constitutes the first report on the cloning and characterization of the terpenoid biosynthetic pathway genes DXS, DXR, CMK, MCS, HDS, HDRs, HMGRs, MK, PMK, and MVD from *P. umbrosa*. In addition, we detected terpenoid accumulation in different organs of this species. The expression of transcripts of *PuHMGR1, PuHMGR2,* and *PuMVD* was the highest in the root tissues, where sesamoside and shanzhiside methylester were also more abundant than in other organs. However, in terms of the gene expression level, *PuHMGR* plays a vital role in the biosynthesis of terpenoids in the roots of *P. umbrosa*. The transcript levels of *PuDXS, PuCMK, PuMCS, PuHDR1,* and *PuHDR2* were the highest in the bud and leaf tissues, and the contents of umbroside and acteoside were also the highest in those tissues. The gene expression profiles of *PuHDR* are believed to play an important role in terpenoid biosynthesis in the buds and leaves. Many studies have shown a relationship between the accumulation of terpenoids and the genes HDR and HMGR, in multiple species [34–37]. The contents of iridoid glycosides, such as sesamoside (0.38 ± 0.87%DW), shanzhiside methylester (0.04 ± 1.07%DW), and acteoside (0.13 ± 4.86%DW), have been reported for the leaves of *Sesamum indicum* [37]. When comparing the total amount of terpenoids, there were many white flower plant in the underground part and pink flower plant in the above-ground part. *P. umbrosa* white flower plants contained five times more Shanzhiside methyl ester than pink flower plant at the root. Therefore, it would be better to select white flower plant when breeding *P. umbrosa* for herbal medicine in the future. We suggest that *PuHMGR* and *PuHDR* may play key roles in terpenoid biosynthesis in *P. umbrosa*. Based on this result, the breeding research team intends to develop a variety with a fixed flower color.

5. Conclusions

The present study aimed to characterize the molecular genetics of the terpenoid biosynthetic pathway in *P. umbrosa*. In this study, *PuDXS*, *PuDXR*, *PuCMK*, *PuMCS*, *PuHDS*, *PuHDR*, *PuHMGR*, *PuMK*, *PuPMK*, and *PuMVD* were cloned and characterized from *P. umbrosa* while using NGS data. We analyzed the transcript levels of the genes using qRT-PCR and quantified the accumulated terpenoids in the various organs of *P. umbrosa* using HPLC. The transcript levels of *PuHMGRs* were the highest in the roots, where sesamoside and shanzhiside methylester content were also found at the highest level. The transcript levels of *PuHDRs* and contents of umbroside and acteoside were the highest in the bud and leaf tissues. Our analysis of *PuHMGR* and *PuHDR* expression profiles indicated that these genes are involved in the biosynthesis of terpenoids. These findings provide a technical framework that is based on which study of the underlying mechanism of terpenoid biosynthesis in the different organs of *P. umbrosa* can proceed.

Supplementary Materials: The following are available online at http://www.mdpi.com/2311-7524/6/4/76/s1, Figure S1: Deduced amino acid multiple sequence alignments of the *PuDXS* with other DXSs; Figure S2: Deduced amino acid multiple sequence alignments of the *PuDXR* with other DXRs; Figure S3: Deduced amino acid multiple sequence alignments of the *PuCMK* with other CMKs; Figure S4: Deduced amino acid multiple sequence alignments of the *PuMCS* with other MCSs; Figure S5: Deduced amino acid multiple sequence alignments of the *PuHDS* with other HDSs; Figure S6: Deduced amino acid multiple sequence alignments of the *PuHDR* with other HDRs; Figure S7: Deduced amino acid multiple sequence alignments of the *PuHMGR* with other HMGRs; Figure S8: Deduced amino acid multiple sequence alignments of the *PuMK* with other MKs; Figure S9: Deduced amino acid multiple sequence alignments of the *PuPMK* with other PMKs; Figure S10: Deduced amino acid multiple sequence alignments of the *PuMVD* with other MVD.

Author Contributions: S.U.P. and Y.B.K. designed the experiments and analyzed the data. S.-Y.H., S.-H.L., Y.-S.L., S.-H.H., B.-H.S. and C.S.R. wrote the manuscript, performed the experiments, and analyzed the data. All authors have read and agreed to the published version of the manuscript.

Funding: This research was funded by the Cooperative Research Program for Agriculture Science & Technology Development (Project No. PJ01131503), Rural Development Administration, Republic of Korea, for providing financial support to carry out this work.

Conflicts of Interest: The authors declare no conflict of interest.

References

1. Zhang, Y.; Wang, Z.Z. Comparative analysis of essential oil componets of three *Phlomis* species in Qinling Mountains of China. *J. Pharm. Miomed. Anal.* **2008**, *47*, 213–217. [CrossRef]
2. Liu, P.; Deng, R.X.; Duan, H.Q.; Yin, W.P.; Zhao, T.Z. Phenylethanoid glycosides from the roots of *Phlomis umbrosa*. *J. Asian Nat. Prod. Res.* **2009**, *11*, 69–74. [CrossRef]
3. Lee, D.; Kim, Y.S.; Song, J.; Kim, H.S.; Lee, H.J.; Guo, H.; Kim, H. Effects of *Phlomis umbrosa* root on longitudinal bone growth rate in adolescent female rats. *Molecules* **2016**, *21*, 461. [CrossRef]
4. Ding, M.M.; Yan, F.L.; Tan, J.; Bai, Y.X.; Wang, X.; Yang, Y.X. Two new dammarane-type glycosides from *Phlomis umbrosa*. *Nat. Prod. Res.* **2014**, *28*, 18–23. [CrossRef]
5. Shin, T.Y.; Kim, S.H.; Kim, D.K.; Leem, K.H.; Park, J.S. *Phlomis umbrosa* root inhibits mast cell-dependent allergic reactions and inflammatory cytokine secretion. *Phytother. Res.* **2008**, *22*, 153–158. [CrossRef] [PubMed]
6. Shang, X.; Wang, J.; Li, M.; Miao, X.; Pan, H.; Yang, Y.; Wang, Y. Anti-nociceptive and anti-inflammatory activities of *phlomis umbrosa* turcz extract. *Fitoterapia* **2011**, *82*, 716–721. [CrossRef]
7. Breitmaier, E. Terpenes: Flavors, Fragrances, Pharmaca, Pheromones. In *Terpene: Importance, General Structure, and Biosynthesis*; Wilely–VCH: Weinheim, Germany, 2006; pp. 2–3.
8. Inouye, H.; Takeda, Y.; Nishmura, H.; Kanomi, A.; Okuda, T.; Puff, C. Chemotaxonomic studies of Rubiaceous plants containing iridoid glycosieds. *Phytochemistry* **1988**, *27*, 2591–2598. [CrossRef]
9. Alpieva, K.I.; Taskova, R.M.; Evstatieva, L.N.; Handjieva, N.V.; Popov, S.S. Benzoxazinoids and iridoid glucosides from four *Laminum* species. *Phytochemistry* **2003**, *64*, 1413–1417. [CrossRef]
10. Zhao, Y.Y.; Guo, L.; Cao, L.J.; Zhang, J.; Yin, Z.Q. A new iridoid glycoside from the fruits of *Vitex rotundifolia*. *Nat. Prod. Res.* **2017**, *31*, 2491–2496. [CrossRef]

11. Fan, P.C.; Ma, H.P.; Hao, Y.; He, X.R.; Sun, A.J.; Jiang, W.; Li, M.X.; Jing, L.L.; He, L.; Ma, J.; et al. A new anti-fibrinolytic hemostatic compound 8-O-acetyl shanzhiside methylester extracted from *Lamiopholomis rotata*. *J. Ethnopharmacol.* **2016**, *187*, 232–238. [CrossRef]
12. Cui, Y.; Wang, Y.; Zhao, D.; Feng, X.; Zhang, L.; Liu, C. Loganin prevents BV-2 microglia cells from $A\beta_{1\text{-}42}$-induced inflammatiion via regulating TLR4/TRAF-κB axis. *Cell Biol. Int.* **2018**, *42*, 1632–1642. [CrossRef]
13. Czerwinska, M.E.; Swierczewska, A.; Granica, S. Bioactive constituents of *Lamium album* L. as inhibitors of cytokine secretion in human neutrophils. *Molecules* **2018**, *23*, 2770. [CrossRef]
14. Webb, H.; Foley, W.J.; Külheim, C. The genetic basis of foliar terpene yield: Implications for breeding and profitability of Australian essential oil crops. *Plant. Biotechnol.* **2014**, *31*, 363–376. [CrossRef]
15. Sun, W.J.; Zhan, J.Y.; Zheng, T.R.; Sun, R.; Wang, T.; Tang, Z.Z.; Bu, T.L.; Li, C.L.; Wu, Q.; Chen, H. The jasmonate-responsive transcription factor *CbWRK24* regulates terpenoid biosynthetic genes to promote sapnin biosynthesis in *Conyza blinii* H. Léb. *J. Genet.* **2018**, *97*, 1379–1388. [CrossRef]
16. Yu, N.; Yang, J.C.; Yin, G.T.; Li, R.S.; Zou, W.T. Transcriptome analysis of oleoresin-producing tree *Sindora Glabra* and characterizationof sesquiterpene synthases. *Front. Plant Sci.* **2018**, *9*, 1619. [CrossRef]
17. Zhang, H.; Jin, B.; Bu, J.; Guo, J.; Chen, T.; Ma, Y.; Tang, J.; Cui, G.; Huang, L. Transcriptomic insight into terpenoid biosynthesis and functional characterizaion of three diterpene synthases in *Scutellaria barbata*. *Molecules* **2018**, *23*, 2952. [CrossRef]
18. Ali, M.; Hussain, R.M.; Rehman, N.U.; She, G.; Li, P.; Wan, X.; Guo, L.; Zhao, J. *De novo* transcriptome sequencing and metabolite profiling analysis reveal the comples metabolic genes involved in the terpenoid biosynthesis in blue anise sage (*Salvia guaranitica* L.). *DNA Res.* **2018**, *25*, 597–617. [CrossRef]
19. Park, Y.J.; Arasu, M.V.; Al-Dhabi, N.A.; Lim, S.S.; Kim, Y.B.; Lee, S.W.; Park, S.U. Expression of terpenoid biosynthetic genes and accumulation of chemical constituents in *Valeriana fauriei*. *Molecules* **2016**, *21*, 691. [CrossRef]
20. Li, M.; Zhang, C.; Wei, L.; Fan, P.; Zhang, Q.; Jia, Z. Determination of five iridoid glycosides in *Phlomis younghusbandii* by HPLC. *China J. Chin. Mater. Med.* **2011**, *36*, 594–597.
21. Sprenger, G.A.; Schörken, U.; Wiegert, T.; Grolle, S.; de Graaf, A.A.; Taylor, S.V.; Begley, T.P.; Bringer-Meyer, S.; Sahm, H. Identification of a thiamin-dependent synthase in *Escherichia coli* required for the formation of the 1-deoxy-D-xylulose 5-phosphate precursor to isoprenoids, thiamin, and pyridoxol. *Proc. Natl. Acad. Sci. USA* **1997**, *94*, 12857–12862. [CrossRef]
22. Yao, H.; Gong, Y.; Zuo, K.; Ling, H.; Qiu, C.; Zhang, F.; Wang, Y.; Pi, Y.; Liu, X.; Sun, X.; et al. Molecular cloning, expression profiling and functional analysis of *DXR* gene encoding 1-deoxy-D-Xylulose 5-phosphate reductoisomerase from *Camptotheca acuminata*. *J. Plant Physiol.* **2008**, *165*, 203–213. [CrossRef]
23. Rohdich, F.; Wungsintaweekul, J.; Lüttgen, H.; Fischer, M.; Eisenreich, W.; Schuhr, C.A.; Fellermeier, M.; Schramek, N.; Zenk, M.H.; Bacher, A. Biosynthesis of terpenoids: 4-Diphosphocytidyl-2-*C*-methyl-D-erythritol kinase from tomato. *Proc. Natl. Acad. Sci. USA* **2000**, *97*, 8251–8256. [CrossRef] [PubMed]
24. Kim, S.M.; Kuzuyama, T.; Chang, Y.J.; Kim, S.U. Cloning and characterizatiion of 2-*C*-methyl-D-erythritol 2,4-cyclodiphosphate synthase (MECS) gene from *Ginkgo biloba*. *Plant Cell Rep.* **2006**, *25*, 829–833. [CrossRef]
25. Wolff, M.; Seemann, M.; Grosdemange-Billiard, C.; Tritsch, D.; Campos, N.; Rodriguez-Concepción, M.; Boronat, A.; Rohmer, M. Isoprenoid biosynthesis via the methylerythritol phosphate pathway. *(E)*-4-Hydroxy -3-methylbut-2-enyl diphosphate: Chemical synthesis and formation from methylerythritol cyclodiphosphate by a cell-free sstem from *Escherichia coli*. *Tetrahedron Lett.* **2002**, *43*, 2555–2559. [CrossRef]
26. Hsieh, W.Y.; Hsieh, M.H. The amino-terminal conserved domain of 4-hydroxy-3-methylbut-2enyl diphosphate reductase is critical for its function in oxygen-evolving photosynthetic organisms. *Plant Signal. Behav.* **2015**, *10*, e988072. [CrossRef]
27. Istvan, E.S. Bacterial and mamalian HMG-CoA reductases: Related enzymes with distinct architectures. *Curr. Opin. Struc. Biol.* **2001**, *11*, 746–751. [CrossRef]
28. Andeassi, J.L., 2nd.; Bilder, P.W.; Vetting, M.W.; Roderick, S.L.; Leyh, T.S. Crystal structure of the *streptococcus pneumoniae* mevalonate kinase in complex with diphosphomevalonate. *Protein Sci.* **2007**, *16*, 983–989. [CrossRef]
29. Doun, S.S.; Burgner, J.W., 2nd.; Briggs, S.D.; Rodwell, V.W. *Enterococcus faecalis* phosphomevalonate kinase. *Protein Sci.* **2005**, *14*, 1134–1139. [CrossRef]

30. Cordier, H.; Lacombe, C.; Karst, F.; Bergès, T. The *Saccharomyces cerevisiae* mevalonate diphosphate decarboxylase (*Erg19p*) forms homodimers in vivo, and a single substitution in a structurally conserved region impairs dimerization. *Curr. Microbiol.* **1999**, *38*, 290–294. [CrossRef]
31. Xu, C.; Li, H.; Yang, X.; Gu, G.; Mu, H.; Yue, Y.; Wang, L. Cloning and expression analysis of MEP pathway enzyme-encoding genes in *Osmanthus fragrans*. *Genes* **2016**, *7*, 78. [CrossRef] [PubMed]
32. Lv, J.; Liu, G.S.; Hussian, Z.; Sun, Y.H. Cloning and expression analysis of terpenoid metabolism-related gene *NsyCMS* in *Nicotiana sylvestris*. *Genet. Mol. Res.* **2015**, *14*, 3300–3308. [CrossRef]
33. Souret, F.F.; Kim, Y.; Wyslouzil, B.E.; Wobbe, K.K.; Weathers, P.J. Scale-up of *Artemisia annua* L. hairy root cultures produces complex patterns of terpenoid gene expression. *Biotechnol. Bioeng.* **2003**, *83*, 653–667. [CrossRef] [PubMed]
34. Dai, Z.; Cui, G.; Zhou, S.F.; Zhang, X.; Huang, L. Cloning and characterization of a novel 3-hydroxy-3 -methylglutaryl coenzyme A reductase gene from Salvia miltiorrhiza involved in diterpenoid tanshinone accumulation. *J. Plant Physiol.* **2011**, *168*, 148–157. [CrossRef]
35. Xu, J.W.; Xu, Y.N.; Zhong, J.J. Enhancement of ganoderic acid accumulation by overexpression of an N-terminally truncated 3-hydroxy-3-methylglutaryl coenzyme A reductase gene in basidomycete *Ganoderma lucidum*. *J. Appl. Environ. Microbiol.* **2012**, *78*, 7968–7976. [CrossRef] [PubMed]
36. Martin, D.M.; Chiang, A.; Lund, S.T.; Bohlmann, J. Biosynthesis of wine aroma; transcript profiles of hydroxymethybutenyl diphosphate reductase, geranyl diphosphate synthase, and linalool/nerolidol synthase parallel monoterpenol glycoside accumulation in gewürztraminer grapes. *Planta* **2012**, *236*, 919–929. [CrossRef]
37. Fuji, Y.; Uchida, A.; Fukahori, K.; Chino, M.; Ohtsuki, T.; Matsufuji, H. Chemical characterization and biological activity in young sesame leaves (*Sesamum indicum* L.) and changes in iridoid and polyphenol content at different growth stages. *PLoS ONE* **2018**, *13*, e0194449. [CrossRef] [PubMed]